Experimental Observation of Low Noise and Low Drift in a Laser-Driven Fiber Optic Gyroscope

Seth W. Lloyd, Shanhui Fan, *Fellow, IEEE*, and Michel J. F. Digonnet

***Abstract*—We demonstrate that by driving a fiber optic gyroscope (FOG) with a laser of relatively broad linewidth ($\sim 10\,\mathrm{MHz}$), both the noise and the bias drift are reduced to very low levels ($0.058°/\sqrt{\mathrm{h}}$ and $1.1°/\mathrm{h}$, respectively), comparable to the performance of the same gyroscope conventionally driven with a broadband light source. When the laser linewidth is reduced to a low enough value ($\sim 2.2\,\mathrm{kHz}$), the FOG exhibits a higher drift but an even lower noise, about 4 dB lower than with a broadband source, and only 3.5 dB above shot noise. The measured dependencies of the noise and drift on laser linewidth are in good quantitative agreement with the predictions of an advanced model of backscattering errors in a FOG interrogated with coherent light, which confirms that the noise and drift are predominantly limited by backscattering. The use of a laser comes with the additional benefit of a much greater wavelength stability compared to a broadband source, which is expected to translate directly into a much more stable scale factor than possible in conventional FOGs. Residual sources of drift and the prospects for reducing them in order to achieve inertial navigation performance are discussed.**

***Index Terms*—Backscattering drift, backscattering noise, coherent backscattering, fiber optic gyroscope, laser phase noise, Sagnac interferometer.**

I. Introduction

FIBER optic gyroscopes (FOGs) have been an active area of research since they were first proposed for rotation sensing in 1976 [1]. Following intense research in the 1980s and early 1990s, modern FOGs now achieve performance, across most important metrics, on par with or exceeding the performance of competing inertial navigation technologies, such as ring laser gyroscopes. The sole primary metric where FOGs continue to lag is the scale-factor stability, which is impaired by instability in the mean wavelength of the broadband sources used for interrogating FOGs. In a high-end FOG, the scale-factor stability is typically roughly one order of magnitude worse than competing optical gyroscope technologies [2].

Because the spectrum of a laser can be stabilized to a much higher degree than that of the broadband sources used in a FOG, this instability issue could be solved by interrogating a FOG with a laser. The use of a laser would also lower the cost of the source, consume less electrical power, and be simpler to manufacture. The drawbacks of using a laser, demonstrated by early FOG prototypes evaluated in the 1970s and 1980s, are that coherent light introduces three significant sources of noise and/or drift, namely coherent backscattering, [3], [4] Kerr-induced drift, [5] and polarization non-reciprocities [4], [6]. These errors were the reason why lasers were abandoned in the 1980s and universally replaced by temporally incoherent light sources, especially the Er-doped superfluorescent fiber source (SFS).

In intervening years, in part thanks to the optical communication revolution of the 1990s, several significant technological improvements have been made that lead us to believe a laser may now be a suitable source for the FOG. First, more accurate and reliable optical components such as lasers are now available. In particular, semiconductor lasers around 1.5 $\mu\mathrm{m}$ have a frequency stability that far exceeds the 1 part-per-million (ppm) level required for the scale factor stability of FOGs targeting aircrafts inertial-navigation applications. Progress in the $\mathrm{LiNbO_3}$ multi-function integrated optic circuits (MIOCs) developed for commercial FOGs have also led to MIOC couplers with a coupling ratio much closer to the ideal value of 50%, which implies much reduced Kerr-induced drift. MIOCs also now have polarizers with exceedingly high extinction ratios ($> 80\,\mathrm{dB}$) [7], which is expected to translate into far weaker errors due to polarization non-reciprocities. The use of 1.5-$\mu\mathrm{m}$ light instead of the shorter wavelengths used in early laser-driven FOGs also implies reduced coherent-backscattering errors.

Of these three error mechanisms, we believe that coherent backscattering due to randomly distributed defects in the sensing fiber is likely to be the dominant one. To assess the magnitude of the noise and drift caused by backscattering, we recently developed a rigorous theoretical model that quantifies these two errors in a FOG interrogated by a source of arbitrary coherence length [8]. This model showed, for the first time, that coherent-backscattering errors are not nearly as large as anticipated by an earlier model [3], and that by proper choice of the coherence length of the laser and of the applied modulation, both errors can be reduced in principle to below inertial-navigation requirements. As a proof of concept, we recently reported the first laser-driven FOG with a lower experimental noise than the noise of the same FOG driven with an SFS [9].

In this paper, we provide the first experimental quantitative verifications of these predictions, in particular of the predicted dependence of the noise and of the drift induced by backscattering on the coherence length of the laser. By driving our FOG with a laser of relatively broad linewidth, we demonstrate for the first time a laser-driven FOG with both a noise and a long-term drift comparable to the same gyroscope driven with a broadband

Manuscript received December 06, 2012; revised February 26, 2013; accepted March 23, 2013. Date of publication May 06, 2013; date of current version May 31, 2013. This work was supported in part by Litton Systems, Inc., a wholly owned subsidiary of Northrop Grumman Corporation.

The authors are with Stanford University, Stanford, CA 94305-4085 USA (e-mail: swlloyd@stanford.edu; shanhui@stanford.edu; silurian@stanford.edu).

Color versions of one or more of the figures in this paper are available online at http://ieeexplore.ieee.org.

Digital Object Identifier 10.1109/JLT.2013.2261285

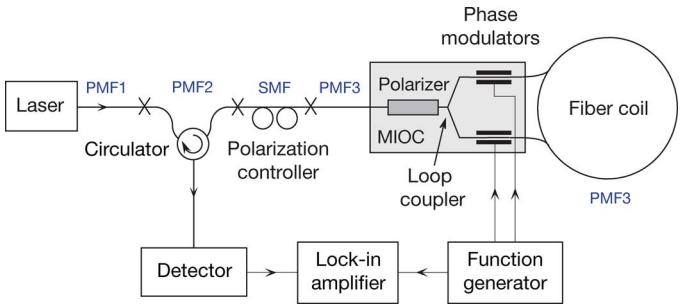

Fig. 1. Experimental laser-driven FOG.

source. When the source is replaced with a narrow-linewidth laser, the FOG exhibits a higher drift but an even lower noise, about 4 dB lower than with a broadband source, and only 3.5 dB above shot noise. These results validate a critical new concept, namely that operating a FOG with a laser of judiciously chosen linewidth can lead to noise and drift performance comparable to or better than with a broadband source. These improvements come hand in hand with the far greater wavelength stability of a laser compared to a broadband source, which is expected to translate directly into a much greater scale-factor stability than is currently achievable with a broadband source.

II. Experimental Laser-Driven Fiber Optic Gyroscope

To measure the impact of laser coherence on coherent-backscattering noise and drift in a FOG, we used the open-loop gyroscope depicted in Fig. 1. The sensing-fiber coil was made of 150-m of high-birefringence polarization-maintaining (PM) fiber wound in a quadrupolar pattern to minimize thermal drift due to the Shupe effect. The coil diameter was 3.5 cm. To form the Sagnac interferometer, the coil was closed upon itself using a $LiNbO_3$ MIOC. This optical circuit incorporated a nominally 50% loop Y coupler, a polarizer, and two phase modulators. The phase modulators were operated in a push-pull configuration using sinusoidal modulation at the loop proper frequency ($f_m = 666 \pm 0.1$ kHz, as determined experimentally), with a modulation amplitude of ~ 0.46 rad per modulator for maximum sensitivity. Three kinds of PM fibers were involved in this prototype: PMF1 (see Fig. 1) in the pigtail of the laser, PMF2 in the pigtails of the circulator, and PMF3 in the pigtail of the MIOC and the Sagnac coil. The cladding diameters were 125 μm for PMF1 and PMF2, and 80 μm for PMF3. To achieve low noise and drift in this gyroscope, it was critical that the splices between these fibers were of high quality in order to minimize the spurious reflection at the interface between the (dissimilar) fibers, and hence minimize coherent errors due to these reflections [8]. It was also important to achieve precise orientation of the fiber's principal axes, to minimize errors due to polarization non-reciprocities [4]. Meeting these objectives was relatively straightforward for the splice between PMF1 and PMF2 (see Fig. 1) using a conventional PM-fiber fusion splicer. However, this proved to be significantly more challenging for the splice between PMF2 and PMF3 because of their different diameters. This problem was circumvented by inserting a short ($\sim$ 30-cm) piece of conventional non-PM SMF-28 fiber between PMF2 and PMF3 (labeled SMF in Fig. 1), which eliminated the need for precise angular alignment. To ensure that the light incident from SMF onto PMF3 was aligned with a principal axis of PMF3, a fiber polarization controller was placed on SMF, and adjusted for maximum return power at the start of each measurement.

The noise and drift of this FOG were characterized when it was interrogated with either a broadband Er-doped SFS or a laser. Three commercial lasers with very different linewidths were evaluated: a laser from Redfern Integrated Optics with a narrow linewidth of 2.2 kHz, a laser from Santec with a 200-kHz linewidth, and a 10-MHz DFB telecom laser from Lucent. These sources had a nominal center wavelength of 1.55 μm. The FOG output was demodulated using a lock-in amplifier synchronized to the modulation frequency. For all reported measurements the filter in the lock-in-amplifier was set to have a roll-off of 24 dB/octave, which means that the effective detection bandwidth was related to the integration time τ set on the lock-in amplifier by $\Delta\nu = 5/(64\tau)$. For Allan variance measurements, the roll off was 6 dB/octave, giving an effective bandwidth $\Delta\nu = 1/4\tau$.

III. Predicted Backscattering Noise and Drift

As a brief summary of the theoretical model of the noise and drift caused by backscattering in a FOG interrogated with a laser of arbitrary linewidth, we reproduce in Fig. 2 the predictions made in [8]. The solid curves represent the results of numerical simulations carried out for the experimental FOG of Fig. 1 with the physical parameter values mentioned in Section II. Fig. 2(a) plots the predicted noise as a function of laser linewidth $\Delta\nu$, from a highly coherent laser ($\Delta\nu = 1$ kHz, or a coherence length in the fiber of ~ 66 km) to a laser of fairly low coherence ($\Delta\nu = 10$ MHz, or $L_c = 6.6$ m). As explained in greater detail in [8], when L_c is short only the scatterers located $\pm L_c/2$ on either side of the Sagnac loop's midpoint contribute to coherent backscattering. The other scatterers along the rest of the loop contribute to intensity noise, which is negligible. As L_c is increased the number of coherent backscatteres increases, and the noise increases (see Fig. 2). When L_c reaches the value of the loop length L, all the scatterers that exist in the loop contribute to coherent noise, and the noise is maximum. Increasing the coherence length further, however, leads to a decrease in noise because the laser linewidth decreases, and hence the laser phase noise also decreases, and so does coherent backscattering (which is driven by phase noise) [8].

Fig. 2(b) plots an upper bound of the expected drift due to backscattering [8]. The same increase in drift is observed as the coherence length increases from short values (right side of the graph) to the loop length L. But when L_c exceeds L the drift remains high because it is a measure of the total power backscattered by the fiber, which is maximum when $L > \sim L_c$, as opposed to the noise, which is a measure of the fluctuations in this backscattered power [8]. One of the key objectives of the work reported here was to verify these two dependencies experimentally.

IV. Measured Performance

The noise (random walk) and drift of the laser-driven FOG were calculated from measured temporal output traces of the FOG using the Allan variance method, the standard technique

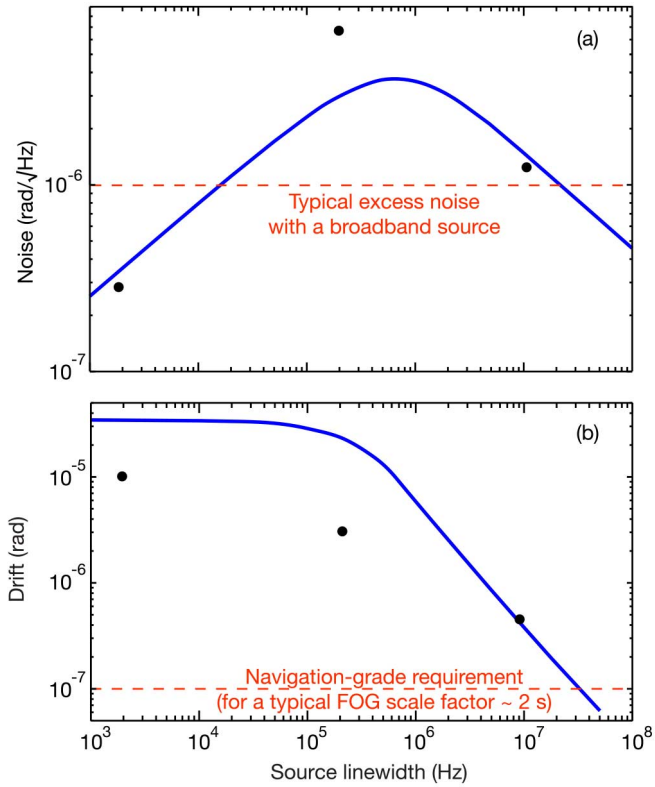

Fig. 2. (a) Angular random walk and (b) bias error calculated for the laser-driven FOG of Fig. 1. Solid dots are experimental data points.

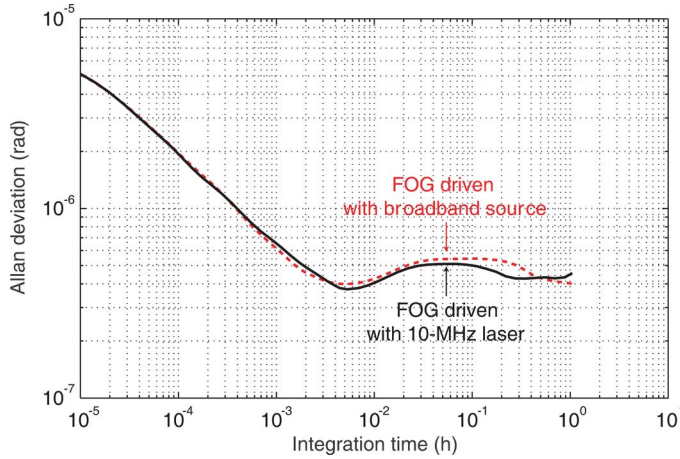

Fig. 3. Measured Allan deviation curve for the fiber optic gyroscope driven with the l0-MHz laser (black curve) or the broadband light source (red dashed curve).

used for characterizing gyroscopes and other instruments [10]. To generate a composite Allan variance plot, for each laser two measurements were performed. The first one recorded the output voltage of the lock-in amplifier over a 15-min period at a sampling rate of $\sim$ 100 Hz. The effective bandwidth of the lock-in amplifier was chosen to ensure that no portion of the signal was aliased when sampling at the chosen rate. This bandwidth was typically $\Delta\nu = 25$ Hz. The second measurement was taken over a longer period, generally 12 h. The sampling rate was reduced to $\sim$ 1 Hz, and the effective bandwidth was similarly adjusted (to typically $\Delta\nu = 0.25$ Hz) to avoid aliasing and reduce the volume of data collected. For both measurements, the FOG was in a largely uncontrolled environment, although the coil, MIOC, and circulator were placed inside a small thermal container that provided some thermal and acoustic isolation. The coil was maintained at rest in the laboratory environment, with its axis perpendicular to the optical bench. The data from both measurements was processed using a standard Allan variance algorithm. [10] The two separate Allan variance plots were then combined to form a single plot covering integration times ranging from 10^{-5} h to 1 h.

The black curve in Fig. 3 shows the Allan deviation measured in this fashion in the FOG interrogated with the 10-MHz DFB laser. These measurements were carried out at a detected power level of 20 μW. For short integration times, the curve is linear with a slope of $-1/2$, indicating that the sensor noise is dominated by white noise, as expected. At any point along this linear region, the ratio of ordinate to abscissa is constant and a measure of the random-walk noise of the gyroscope, which in this case is 1.2 $\mu\mathrm{rad}/\sqrt{\mathrm{Hz}}$. For longer time constants, the slope of the curve decreases and the curve eventually flattens out, with a slope of zero. The Allan deviation at this minimum is a measure of bias stability. This minimum occurs at ~ 0.38 μrad, and for an integration time of $\sim 5.5 \cdot 10^{-3}$ h, or $\sim$ 20 s. (The value shown for the 10-MHz laser in Fig. 2(b) is a little higher than this ($\sim$ 5 μrad) because it is the value at the local maximum that occurs past the minimum (see Fig. 3), which we feel is a more accurate representation of the long-term drift.) While not shown in Fig. 3, early results for integration times longer than 1 hour show that the Allan variance curve appears to increase with a slope of $+1/2$. This indicates rate random walk (RRW), [10] a sign of greater instability in the output.

For comparison, Fig. 3 also shows the Allan deviation curve measured using the same two-step measurement when the FOG was driven with an Er-doped SFS having a 3-dB bandwidth of roughly 30 nm. The detected power level was kept the same as in laser measurements (20 μW). The laser-driven FOG (black curve) and the broadband source driven FOG (red dashed curve) are almost identical across the entire range of integration times. This demonstrates for the first time that by driving a FOG with a laser of sufficiently broad linewidth, a noise and a drift comparable to that of the same gyroscope driven with a broadband source can be achieved. This result also indicates that the bias stability of the FOG operated with the 10-MHz laser is not limited by coherent effects, but by effect(s) independent of the source coherence. Since the FOG was running in an open-loop configuration, the most likely source of bias instability is the electronic components that modulate and demodulate the signal. Using well-known techniques to operate this FOG with closed-loop signal processing should reduce this electronic drift and lower the overall observed sensor drift.

Similar plots were generated for the two other lasers. From each of the Allan variance plots, the random walk noise and the FOG drift were extracted as explained above for the 10-MHz laser. Fig. 2 plots these measured values as solid dots for all three lasers. These experimental values are in good agreement with the predicted values, thus confirming the predictions of the effects of backscattering in a FOG. Note in particular that because of the statistical nature of the distribution of scatterers

in the sensing fiber, which vary from fiber to fiber, the noise and drift curves of Fig. 2(a) and (b) represent a mean. In practice, as discussed in [8], each of these two curves has a certain width in the vertical direction. In addition, Fig. 2(b) represents an upper bound (overestimation) of the drift dependence on coherence length. It is therefore expected that (1) the measured data points for the noise do not exactly match the theoretical curve of Fig. 2(a), and (2) that the data points for the drift lie below the curve of Fig. 2(b). In spite of these expected departures, the measured data points confirm the previously unpredicted dependence of the noise and drift on source coherence length.

At 1 $\mu\mathrm{rad}/\sqrt{\mathrm{Hz}}$, the noise observed with this linewidth is comparable to typical noise levels for FOGs driven with a broadband source [11]. Furthermore, the measured drift of 0.38 $\mu\mathrm{rad}$ is the first reported experimental observation of a laser-driven FOG with such a low drift. This measured drift includes not just drift caused by backscattering, but also any additional components caused by polarization non-reciprocities and Kerr nonlinearity. This measurement therefore verifies that errors due to these effects are significantly reduced through the combination of modern components, appropriate choice of laser linewidth, and the additional engineering techniques discussed.

To verify experimentally the noise contributions in the laser-driven FOG, we measured the equivalent phase noise at the output of the FOG as the power circulating in the coil was varied by placing an attenuator after the source and before the circulator. The noise values were calculated from 5-s output traces. The observed noise was essentially white for both the SFS and the 2.2-kHz laser. Fig. 4 plots the measured dependence of this noise on the average detected power when the FOG was operated with the SFS (black stars) and with the 2.2-kHz laser (red open circles). The solid curves are the calculated individual contributions from the four dominant noise sources, namely shot noise and detector thermal noise (common and identical for both the SFS-driven and the laser-driven FOGs), excess noise (for the SFS-driven FOG only), and backscattering noise (for the laser-driven FOG only). The backscattering noise contribution is the value predicted by our model and shown in Fig. 2(a) for the 2.2-kHz laser ($\sim$ 0.32 $\mu\mathrm{rad}/\sqrt{\mathrm{Hz}}$). The noise-equivalent power (NEP) for the shot noise (in $\mathrm{mW}/\sqrt{\mathrm{Hz}}$) was calculated using $N_{sh} = (2qP_d/\rho)^{1/2}$, where q is the electron charge, P_d the detected power, and ρ the detector responsivity. This expression was then converted into a phase error (in $\mathrm{rad}/\sqrt{\mathrm{Hz}}$) using the FOG's measured calibrated response (in mW/rad). The detector thermal noise was calculated from its NEP supplied by the manufacturer (2.5 $\mathrm{pW}/\sqrt{\mathrm{Hz}}$), which was divided by the calibrated response to obtain the phase error. The excess noise was calculated using the standard expression. [12] In Fig. 4 the top dashed curve is the predicted total noise for the SFS-driven FOG, i.e., the sum of the three main noise contributions (shot noise, detector noise, and excess noise), assumed to be independent random variables and therefore summed as the square root of the sum of the three contributions squared. The middle dashed curve is the total noise for the laser-driven FOG, i.e., the sum of the shot noise, detector noise, and backscattering noise.

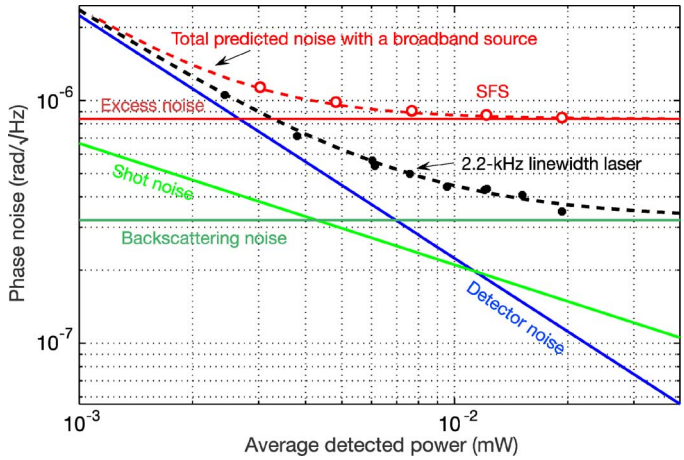

Fig. 4. Measured noise dependence on detected power for the FOG interrogated with either the 2-kHz laser or a broadband source (SFS). The solid curves are the calculated contributions to the noise, and the dashed curves the total calculated contributions for both sources.

For low detected powers, in the FOG driven with the SFS the noise is limited by the thermal noise of the trans-impedance amplifier integrated in the detector. As the detected power increases the noise floor is quickly dominated by the excess noise of the SFS. Shot noise is always negligible. There is excellent agreement between the predicted and measured noise dependencies. The noise behavior here is therefore as expected, and it confirms the correctness of our understanding of the noise contributions and their magnitudes in our FOG, and that our instruments were properly calibrated.

In the case of the laser-driven FOG (see Fig. 4), there is also excellent agreement between the measured noise and the predicted total noise, which confirms once again our understanding of the magnitude of the various noise contributions, especially backscattering. At low detected power the measured noise is also limited by detector noise. The main difference is that as the detected power is increased, the noise decreases to much lower levels than with the broadband source because the laser has negligible excess noise, and because the laser linewidth is so narrow that the backscattering noise is also small. For the highest power available from our laser, the noise approaches the backscattering limit. The lowest random walk in Fig. 4 is about 4 dB lower than with the broadband source, and only 3.5 dB above the shot noise. Importantly, this result shows for the first time that it is possible to operate a FOG with a noise lower than the excess-noise limit. This is accomplished by carefully tailoring the coherence length of the laser.

V. Discussion

A. Required Adjustments in Laser-Driven FOG

In order to obtain the optimal performance reported here, it was important to carefully adjust several of the FOG parameters, in the proper order. First, because for reasons explained in Section II a short length ($\sim$ 30 cm) of non-PM fiber had to be inserted between the circulator and the MIOC, the birefringence of this fiber segment had to be adjusted to ensure that the state of polarization (SOP) input into the MIOC was linear and well aligned with the linear polarization state transmitted by

the MIOC. This adjustment is particularly critical when using a laser, because even though the polarization rejection of the MIOC's polarizer is very high (> 80 dB) [7], it is not sufficient on its own to reduce polarization non-reciprocities below the μrad level. It is therefore important to ensure that as little light is injected at the input to the MIOC into the orthogonal polarization rejected by the polarizer. In a second step, the frequency applied to the push-pull phase modulators was adjusted to precisely match the proper frequency of the sensing loop using the square-wave modulation method [4], [13]. We found empirically that this frequency had to be adjusted to an accuracy of about ± 10 Hz. The third step consisted in adjusting the phase between the two inputs to the lock-in amplifier (the FOG signal and the reference signal from the function generator) to ensure maximum rejection of the quadrature signal measured by the lock-in amplifier. These are the same steps typically taken to adjust a fiber optic gyroscope. However, when the FOG is driven with a laser we found that the performance of the FOG was more sensitive to these adjustments, the reason being that the two coherent sources of error (backscattering and polarization non-reciprocities) are much stronger and have a correspondingly greater sensitivity to these parameters.

In addition, as explained in Section II it was important to reduce reflections from the various fiber splices in the FOG's optical circuit. There were no splices inside the Sagnac interferometer, but there were splices between the MIOC and the source and detector. Although these splices were outside of the interferometer, the small amounts of light they reflect still interfere with the signals returning from the FOG when the laser linewidth is sufficiently narrow (e.g., 2.2 kHz). It was only after reflections from these various fiber junctions had been reduced by optimizing the splices between these dissimilar fibers that the low-noise performance reported above was observed.

The use of push-pull modulation was also instrumental in reducing errors due to coherent backscattering, as justified and predicted through simulations in [8]. When push-pull modulation is combined with a phase-sensitive detection, the detection scheme can be used to filter out a large portion of these errors. While it was known prior to this work that modulating at the proper frequency could reduce backscattering errors for very short coherence lengths (< 100 μm) [14], this earlier analysis only used a single modulator and would have been ineffective for longer coherence lengths. Only by adding an additional modulator and operating in a push-pull configuration could such benefits be extended to longer coherence lengths. The push-pull modulation scheme is almost entirely responsible for reducing the larger drift observed in our earlier work (see for example Fig. 3(b) in [15]).

Finally, utilizing a PM sensing fiber was also an essential step in achieving this low-drift and low-noise performance with a laser interrogation because it greatly reduces polarization nonreciprocities compared to a non-PM fiber. This fact is well-known in FOGs interrogated with a broadband light source [4]. The need for a PM sensing fiber, and in fact an all-PM optical circuit, becomes even more critical in a FOG interrogated with a coherent source.

B. Comparison to Commercial FOGs

To better understand the significance of these results, we list in Table I the random walk (RW) and phase-bias drift measured in the laser-driven FOG investigated here and two commercial tactical-grade gyroscopes, namely a mid-range LN-200 unit from Northrup Grumman and an HG-1900 MEMS gyro from Honeywell. The random walk listed in the table for the laser-driven FOG was obtained by converting the measured random-walk noise of 1.2 $\mu\mathrm{rad}/\sqrt{\mathrm{Hz}}$, which is a phase error, into a rotation-rate error. This was done by dividing the phase error by the scale factor of the gyro, $SF = 0.071$ s, then converting the result from $\mathrm{rad}/\sqrt{\mathrm{s}}$ to $\mathrm{degrees}/\sqrt{\mathrm{h}}$. The same conversion was used to calculate the *rotation-rate* drift shown in Table I (which represents the drift expressed in terms of a rotation-rate error) from the measured phase-bias drift of 0.38 μrad (which represents the drift expressed in terms of a phase error). Both the random walk ($0.058^\circ/\sqrt{\mathrm{h}}$) and the drift ($1.1^\circ/\mathrm{h}$) of our FOG exceed the performance of these two units. While there may be slight differences in definitions and methods of characterization for the various gyros of Table I, it is clear that the laser-driven FOG is capable of performing at a level similar to these commercial tactical-grade units.

TABLE I
COMPARISON OF THE MEASURED NOISE AND DRIFTS OF VARIOUS TACTICAL-GRADE GYROSCOPES AND THE FOG DRIVEN WITH A 10-MHZ LASER DESCRIBED IN THIS WORK

Gyroscope type	RW	Rotation-rate drift
LN-200 311875-240207 [16]	0.15 °/√h	3.0 °/h
HG-1900 BA99 [16]	0.125 °/√h	10 °/h
Laser-driven FOG [this work]	0.058 °/√h	1.1 °/h

It is important to point out that the diameter of the coil used in this FOG is small (3.5 cm), which translates into a small scale factor (0.071 s), and hence an artificially high rotation-rate drift (since the latter is calculated by dividing the phase-bias drift by the scale factor). If a larger coil were to be used, as is typically done in high-accuracy FOGs, the scale factor would be increased, which would result in a lower drift expressed in degrees/hour. This modification would not increase the phase-bias drift due to backscattering, polarization non-reciprocities, or Kerr nonlinearity (since the coil length remains the same). For example, increasing the coil diameter to 17.5 cm would increase the scale factor 5 fold, and thus reduce the rotation-rate drift to $0.22^\circ/\mathrm{h}$. This is ~ 10 to ~ 50 lower than in the two commercial tactical-grade gyroscopes of Table I.

C. Residual Sources of Drift and Mitigation Methods

As mentioned earlier, the most likely source of bias instability in the current prototype is believed to be the electronic components that modulate and demodulate the signal, and closed-loop operation should take care of this issue. Of the other sources of drift, Kerr-induced drift was dismissed as a dominant contribution because the two powers counter-propagating in the coil were less than 35 μW, and the fluctuations between them were measured over several hours of operation to be less than 1%. Calculations based on a proven model [11] show that at this low level of power and fluctuations, the Kerr-induced phase-bias drift is in the range of 0.03–0.04 μrad (the uncertainty comes from the lack of knowledge of the nonlinear constant of the PM fiber). This corresponds to a rotation-rate drift of

0.087–$0.12^\circ/\mathrm{h}$, which is well below ($\sim 10\%$ of) the observed drift. This is confirmed by the experimental observation that the laser-driven and SFS-driven FOGs have the same Allan variance behavior (see Fig. 3). If need be, if the main contributions of drift are successfully reduced to the point where this Kerr-induced drift becomes dominant, the signal input to the coil can be square-wave modulated with a 50% duty cycle to effectively reduce the Kerr-induced drift [5].

Early experiments suggest that the drift observed in the FOG driven with the 10-MHz laser may be in part limited by polarization non-reciprocities, arising in particular from slight misalignments between the eigenpolarization axes of the FOG's various PM components. Experimental and theoretical investigations are being carried out to identify and reduce this contribution.

The rotation-rate drift that is generally deemed acceptable for inertial navigation of aircrafts is $\sim 0.01^\circ/\mathrm{h}$ or below [10]. This is about two orders of magnitude lower than we observed when driving the FOG with the 10-MHz laser (see Table I). As explained in the previous sub-section, a drift of $\sim 0.22^\circ/\mathrm{h}$ can be readily and straightforwardly obtained by winding the coil on a larger mandrel. Increasing the fiber length by a factor of 10 (from the current value of 150 m to 1.5 km) would further increase the scale factor 10 fold, and reduce the rotation-rate drift to $0.022^\circ/\mathrm{h}$, bringing it within a factor of ~ 2 of the navigation-grade requirement. Simple scaling laws derived in [8] show unambiguously that for a laser with such a large linewidth, this increase in fiber length would result in a very small and inconsequential increase in the phase-bias drift due to coherent backscattering. Because the laser's short coherence length ($\sim 6.6\ \mathrm{m}$) is much shorter than the loop length, the Kerr-induced phase-bias drift is proportional to the coherence length, not the loop length, and it would not be increased by this increase in loop length. However, this length increase may increase the phase-bias (and rotation-rate) drift induced by polarization coupling in the coil. This contribution to drift may then become dominant. The rotation-rate drift can therefore not be expected to be decreased simply by increasing the length. Mitigation measures would need to be implemented to reduce the contribution of polarization non-reciprocities.

VI. Conclusions

Driving a FOG with a laser instead of a traditional broadband light source is expected to offer at least one key advantage, which is a significantly increased scale factor stability arising from the far greater frequency stability of a laser. However, driving a FOG with a laser was previously believed to lead to unacceptably large noise and drift due to deleterious effects taking place in the sensing coil, namely coherent backscattering, the Kerr effect, and polarization non-reciprocity. In this work, we have shown that by using modern components, carefully selecting the laser linewidth, and employing a symmetric phase modulation scheme, these sources of error can be reduced to far lower levels than previously thought possible. By driving the FOG with a laser of relatively broad linewidth (10 MHz), both a low noise ($1.2\ \mu\mathrm{rad}/\sqrt{\mathrm{Hz}}$) and a low drift ($0.38\ \mu\mathrm{rad}$) were demonstrated, a performance comparable to that of the same gyroscope driven with a broadband source. When interrogated with a laser of narrow linewidth (2.2 kHz) instead, the FOG exhibits a higher drift but an even lower noise, about 4 dB lower than the same FOG interrogated with a broadband source, and only 3.5 dB above shot noise. The measured dependence of the noise and drift on the laser linewidth are in good agreement with the predictions of a numerical model of backscattering errors in a FOG, which confirm that these errors are dominated by coherent backscattering. Polarization-induced drift is anticipated to have a similar magnitude, although additional studies are required to determine its magnitude precisely. Importantly, these performances are accomplished with a laser, a light source that has a much greater frequency stability than a broadband source, hence the scale-factor stability of these laser-driven gyroscopes can reasonably be expected to be much greater than has been possible so far with a broadband source.

These results reverse the conventional wisdom that has prevailed for the past three decades. They validate the far-reaching new concept that through careful selection of the laser coherence, a FOG can be driven with a laser to significantly reduce its noise and improve its scale-factor stability. Although in the FOG reported here the drift is still too high for inertial navigation of aircrafts, this study clearly points to straightforward directions to reduce it markedly. The drift induced by coherent backscattering can be reduced by using a laser with an even shorter coherence length. The rotation-rate drift can be reduced by a factor of ~ 5 by winding the coil on a larger mandrel, which will increase the scale factor by the same factor without affecting the phase-bias drift or noise. The rotation-rate drift can also be decreased by an additional factor of ~ 10 by increasing the fiber length 10 fold (to 1.5 km), although this may increase the drift contribution due to polarization non-reciprocities. Meeting the requirement for inertial navigation will therefore likely require evaluating existing and perhaps novel techniques to reduce these polarization effects.

References

[1] V. Vali and R. W. Shorthill, "Fiber ring interferometer," *Appl. Opt.*, vol. 15, no. 5, pp. 1099–1100, May 1976.

[2] H. Lefèvre, "Ultimate-performance fiber-optic gyroscope: A reality," presented at the 16th Opto-Electr. Commun. Conf., Kaohsiung, Taiwan, Jul. 2011.

[3] C. C. Cutler, S. A. Newton, and H. J. Shaw, "Limitation of rotation sensing by scattering," *Opt. Lett.*, vol. 5, no. 11, pp. 488–490, 1980.

[4] H. Lefèvre, *The Fiber-Optic Gyroscope*. Norwood, MA, USA: Artech House, 1993.

[5] R. A. Bergh, H. C. Lefèvre, and H. J. Shaw, "Compensation of the optical Kerr effect in fiber-optic gyroscopes," *Opt. Lett.*, vol. 7, no. 6, pp. 282–284, 1982.

[6] E. C. Kintner, "Polarization control in optical-fiber gyroscopes," *Opt. Lett.*, vol. 6, no. 3, pp. 154–156, 1981.

[7] T. Buret, D. Ramecourt, and F. Napolitano, "From space qualified fiber optic gyroscope to generic fiber optic solutions available for space applications," in *Proc. Int. Conf. Space Optics*, 2008, pp. 14–17.

[8] S. Lloyd, M. J. F. Digonnet, and S. Fan, "Modeling coherent backscattering errors in fiber optic gyroscopes for sources of arbitrary linewidth," *J. Lightw. Technol.*, submitted for publication.

[9] S. W. Lloyd, M. J. F. Digonnet, and S. Fan, "Near shot-noise-limited performance of an open-loop laser-driven interferometric fiber optic gyroscope," in *Proc. Conf. Opt. Fiber Sensors*, Ottawa, Canada, May 2011, vol. 7753, pp. 7753A3-1–A3-4, Postdeadline Paper.

[10] N. El-Sheimy, H. Hou, and X. Niu, "Analysis and modeling of inertial sensors using Allan variance," *IEEE Trans. Instrum. Meas.*, vol. 57, no. 1, pp. 140–149, 2008.

[11] M. J. F. Digonnet, S. Blin, H. K. Kim, V. Dangui, and G. S. Kino, "Sensitivity and stability of an air-core fibre-optic gyroscope," *Meas. Sci. Technol.*, vol. 18, no. 10, pp. 3089–3097, 2007.
[12] P. R. Morkel, R. I. Laming, and D. N. Payne, "Noise characteristics of high-power doped-fibre superluminescent sources," *Electron. Lett.*, vol. 26, no. 2, pp. 96–98, 1990.
[13] H. C. Lefèvre, "Comments about fiber-optic gyroscopes," in *Fiber Optic and Laser Sensors V*, 1987, vol. 838, pp. 86–97.
[14] J. Mackintosh and B. Culshaw, "Analysis and observation of coupling ratio dependence of Rayleigh backscattering noise in a fiber optic gyroscope," *J. Lightwave Technol.*, vol. 7, no. 9, pp. 1323–1328, 1989.
[15] S. Blin, M. J. F. Digonnet, and G. S. Kino, "Fiber optic gyroscope operated with a frequency-modulated laser," in *Proc. Conf. Opt. Fiber Sensors*, Perth, Australia, Apr. 2008, vol. 7004, pp. 70044X-1–4.
[16] J. M. Strus, M. Kirkpatrick, and J. W. Sinko, "Development of a high accuracy pointing system of maneuvering platforms," in *Proc. ION GNSS 20th Int. Tech. Meeting Satellite Division*, 2007, pp. 2541–2549.

Author biographies not included by author request due to space constraints.